INTERNATIONAL JOURNAL FOR NUMERICAL METHODS IN FLUIDS
Int. J. Numer. Meth. Fluids 2010; **62**:1357–1380
Published online 27 May 2009 in Wiley InterScience (www.interscience.wiley.com). DOI: 10.1002/fld.2076

Influence of reaction mechanisms, grid spacing, and inflow conditions on the numerical simulation of lifted supersonic flames

P. Gerlinger[1,*,†], K. Nold[2] and M. Aigner[2]

[1]*Institut für Verbrennungstechnik der Luft- und Raumfahrt, Universität Stuttgart, 70569 Stuttgart, Germany*
[2]*Institut für Verbrennungstechnik, DLR VT, Stuttgart, Germany*

SUMMARY

The simulation of supersonic combustion requires finite-rate chemistry because chemical and fluid mechanical time scales may be of the same order of magnitude. The size of the chosen reaction mechanism (number of species and reactions involved) has a strong influence on the computational time and thus should be chosen carefully. This paper investigates several hydrogen/air reaction mechanisms frequently used in supersonic combustion. It is shown that at low flight Mach numbers of a supersonic combustion ramjet (scramjet), some kinetic schemes can cause highly erroneous results. Moreover, extremely fine computational grids are required in the lift-off region of supersonic flames to obtain grid-independent solutions. The fully turbulent Mach 2 combustion experiment of Cheng *et al.* (*Comb. Flame* 1994; **99**: 157–173) is chosen to investigate the influences of different reaction mechanisms, grid spacing, and inflow conditions (contaminations caused by precombustion). A detailed analysis of the experiment will be given and errors of previous simulations are identified. Thus, the paper provides important information for an accurate simulation of the Cheng *et al.* experiment. The importance of this experiment results from the fact that it is the only supersonic combustion test case where temperature and species fluctuations have been measured simultaneously. Such data are needed for the validation of probability density function methods. Copyright © 2009 John Wiley & Sons, Ltd.

Received 8 January 2008; Revised 24 March 2009; Accepted 25 March 2009

KEY WORDS: scramjet; turbulence chemistry interaction; supersonic combustion; detached flame; kinetic scheme; turbulent combustion; ignition delay; hydrogen

1. INTRODUCTION

The development of scramjets strongly depends on numerical simulation because realistic combustor entrance conditions are hard to achieve in ground test facilities and flight tests are

*Correspondence to: P. Gerlinger, Institut für Verbrennungstechnik, DLR VT, Pfaffenwaldring 38-40, 70569 Stuttgart, Germany.
†E-mail: peter.gerlinger@dlr.de

Contract/grant sponsor: EU; contract/grant number: AST4-CT-2005-012282

extremely expensive. Up to now only small-subscale combustors have been investigated experimentally, both at the ground level and in flight. Thus, tested and validated numerical codes may bridge the gap between the available experience with subscale combustors and real size engines. The most important factors for an accurate simulation of reactive high-speed flows are a good shock capturing (including shock boundary layer interaction), a good turbulence modeling, a good simulation of compressible mixing, an accurate modeling of turbulence chemistry interaction, and, last but not the least, a good description of the combustion process by the chosen reaction mechanism.

Since finite-rate chemistry is required in supersonic combustion, a large number of species transport equations have to be solved and the set of governing equations becomes numerically stiff. Therefore, implicit numerical solvers are usually required. Chemistry and very fine, high aspect-ratio grid cells near solid walls are reasons for the long computational times of scramjet combustor simulations. Because of the high computational effort, the number of chemical species should be kept as low as possible. On the other hand, small (skeletal) reaction mechanisms may not be able to accurately predict the lift-off heights of flames at conditions close to the ignition limit. Therefore, skeletal or even one-step schemes should be used with care.

Future air-breathing propulsion devices may work in a scramjet mode at flight Mach numbers ranging from about 7 to 15 and more. The velocity in the combustor is kept high (at supersonic speed) to avoid excessive losses due to normal shock waves and to keep the static temperature in the combustor low. This is done with the aim to reduce the amount of dissociated species. The combustor inlet temperature should be kept as low as possible as long as flame holding and self-ignition are not endangered. For flight Mach numbers between 7 and 9, combustor inflow temperatures between 700 and 1200 K and pressures between 0.4 and 3 bar are expected. The exact values depend on the chosen inlet and isolator geometry. Under such conditions self-ignition may become a problem in case of axial fuel injection, e.g. by strut injectors. Moreover, simulations become problematic in that the combustor static pressures and temperatures are close to the self-ignition limit, where the reaction mechanisms have their largest inaccuracies. By approaching the self-ignition limit, the number of sensitive reactions increases and the corresponding rate constants have to be described accurately.

Unfortunately, there are not many experiments available for code validation that realize the described combustor conditions. Especially, experiments where the species and temperature fluctuations have been measured are rare. However, this is required if combustion models that consider turbulent fluctuations have to be validated.

2. REACTION MECHANISMS

In this section ignition delays of reaction mechanisms are first investigated for a perfectly stirred reactor (PSR). There are already a number of papers concerning reaction mechanisms, but to our knowledge there is no comparison of those mechanisms, which are most frequently used in supersonic combustion. In addition to the PSR simulations, the chosen mechanisms will be compared for a practical turbulent supersonic flame.

Most published reaction mechanisms are used and validated for subsonic flames only. Exceptions are the Jachimowski mechanisms from 1988 [1] and 1992 [2]. Because the pressure range in a scramjet combustor is relatively small (between about 0.4 and 3 bar), it is possible to neglect

DOI: 10.1002/fld

Table I. Compared hydrogen/air reaction mechanisms (neglecting nitrogen reactions).

Author, year of publication	Species	Reactions	Validation		
			p (bar)	T (K)	Φ
Jachimowski mod. [1, 3] (1988)	9	19	0.5–2	800–1500	—
Skeletal Jachimowski [4] (1992)	7	7	—	—	—
Jachimowski [2] (1992)	9	19	0.5–2	800–1500	—
Vajda *et al.* [5] (1990)	9	19	—	—	—
O'Conaire *et al.* [6] (2004)	9	21	0.05–87	298–2700	0.2–6
GRI3.0 [7] (2002)	9	29	0.013–10	1000–2500	0.5–5
Marinov *et al.* [8] (1995)	4	1	1	—	0.6–1.1

pressure dependencies of the rate constants, as done by Jachimowski. This is usually impossible if a large pressure range must be covered. Despite the fact that NO_x formation may also be of importance for scramjet engines (as a pollutant), the corresponding reactions are neglected in the present investigation if included in the original scheme. This simplification should have no influence on the results presented in this paper.

The reaction mechanisms tested are summarized in Table I, where the numbers of species and reactions involved as well as the ranges of validation (concerning pressure, temperature, and stoichiometric ratio Φ) are indicated. With the exception of the skeletal Jachimowski scheme [4] and the one-step mechanism of Marinov *et al.* [8] all mechanisms use nine species (H_2, O_2, N_2, H_2O, OH, H, O, HO_2, and H_2O_2), but differ in their number of reactions.

The 1988 Jachimowski mechanism [1] (9-species, 20-steps) is one of the most widely used kinetic schemes in supersonic combustion [3, 9–14]. The original mechanism has been slightly modified as presented by Wilson and MacCormack [3]. In 1992 Jachimowski [2] presented another hydrogen/air mechanism for scramjet application, which, however, is seldom found in the literature. Both schemes are compared in this study. Additionally, a simplified version of the detailed 1988 Jachimowski mechanism is investigated, which is referred to as the skeletal Jachimowski scheme. This mechanism was first used by Gaffney *et al.* [4] and is obtained from the original scheme by neglecting the species HO_2 and H_2O_2 and the subsequent chemical reactions. In this way a 7-species, 7-step kinetic scheme is obtained. The skeletal Jachimowski mechanism is also frequently employed in supersonic combustion [15–18]. The following investigation may help to evaluate under which conditions it is justified to use the skeletal scheme.

The fourth mechanism of Table I has been developed by Vajda *et al.* [5] (1990) and has been used for the simulation of detonation waves [19]. In the present study the rate constants for the backward reactions are calculated from equilibrium coefficients, even if the Arrhenius constants of the backward reactions are given by Vajda *et al.* More recently published are the kinetic schemes of O'Conaire *et al.* [6] (2004) and GRI3.0 [7] (2002). The scheme of O'Conaire *et al.* is based on the mechanism of Mueller *et al.* [20] (1999). It has been validated against experimental data in the ranges of 0.05–87 bar pressure, 298–2700 K temperature and 0.2–6.0 equivalence ratio, respectively. Both, the O'Conaire *et al.* and the underlying Mueller *et al.* mechanism, are widely validated and accepted in subsonic combustion. They are also used frequently for DNS [21–23]. Thus the O'Conaire *et al.* scheme is taken as a reference mechanism in the following studies. In addition to the mechanisms cited in Table I, the kinetic schemes of Li *et al.* [24] and the one created

DOI: 10.1002/fld

at the University of California, San Diego [25] have been studied concerning their induction times. The results closely resembled those of the O'Conaire *et al.* mechanism, which, therefore, is the one shown in the present investigation.

The GRI3.0 mechanism (from the Gas Research Institute) is validated for a similarly broad range of thermodynamic conditions (see Table I). The wide pressure ranges of both mechanisms require the consideration of pressure dependencies for some three body reactions. The GRI3.0 mechanism has been developed for methane combustion, but is also validated for the stoichiometric combustion of hydrogen/air mixtures at pressures of 1 and 2 bar [26] and has been used for supersonic combustion [27].

Finally, the one-step kinetic model $H_2 + 1/2\,O_2 = H_2O$ of Marinov *et al.* [8] is included in the study. One-step reactions are still used for complex flows or LES [28] (large eddy simulations), but are very limited with respect to their thermodynamic range of applicability [29]. The chosen one-step reaction model is validated for 1 bar pressure and was found to achieve good results concerning laminar flame speeds for equivalence ratios between 0.6 and 1.1 [8]. Ignition delays have not been investigated in Ref. [8]. This is accomplished in this paper.

For a supersonic combustor Sung *et al.* [29] observed a non-monotonic behaviour for the self-ignition limit with respect to pressure. It resembles the first and second explosion limits of homogeneous hydrogen/air mixtures. This means that keeping the initial temperature constant while increasing the pressure, the mixture may change from non-ignitable to ignitable and back to non-ignitable. This is due to a competition between chain branching and chain terminating reactions. Such a behaviour cannot be described by a one-step reaction model and it is certainly a limit for any skeletal kinetic scheme.

3. INVESTIGATION OF INDUCTION TIMES

In a first step induction times of the reaction mechanisms given in Table I are calculated for pressures, temperatures, and stoichiometric ratios that are relevant to supersonic combustion. The induction time may be defined in various ways. Starting from a given homogeneous mixture of H_2, N_2, and O_2, it can be defined as the time when the rate of change of temperature or of OH concentration reaches its maximum. Both definitions have been compared for the O'Conaire *et al.* mechanism and the differences were hardly visible. Thus, the maximum rate of temperature change is used.

Induction times have been measured by several authors for diluted hydrogen/air mixtures [30–33]. Table II summarizes the authors and test conditions of six experiments used in the following study. According to the conditions in supersonic combustors, experiments at pressures between 0.43 bar and 4 bar are chosen. The temperatures correspond to combustor inlet temperatures at low scramjet flight Mach numbers and range from 850 to 1320 K. In all cases a dilution of the gas (see Table II) is used for the shock tube experiments. With exception of the Slack data all results are taken from the report of Schultz and Shepherd [34], who created a detailed data base of performed shock tube experiments.

Two different codes have been used for induction time calculations: the in-house code PAD and the free source code CANTERA [35]. The results of both programs correspond very well. CANTERA was finally chosen to perform the subsequent calculations because it is an open source program and because it is able to handle the CHEMKIN input format that is mostly used for the description of reaction mechanisms.

DOI: 10.1002/fld

Table II. Experimental data for the ignition delay time validation.

Author, year of publication	Pressure (bar)	Temperature (K)	Φ	Dilutant N_2 (%)
Just and Schmalz [30] (1977)	0.43	960–1205	1	55.62
Just and Schmalz [30] (1977)	0.45	900–1213	0.1	75.83
Snyder *et al.* [31] (1965)	1	913–967	1	55.62
Snyder *et al.* [31] (1965)	2	857–980	1	55.62
Slack [32] (1977)	2	960–1180	1	55.62
Bhaskaran *et al.* [33] (1973)	2.5	1038–1323	1	55.62
Snyder *et al.* [31] (1965)	4	917–976	1	55.62

For a given initial gas composition, pressure, and temperature unsteady simulations are performed until chemical equilibrium is reached. The chosen constant time step is reduced until a time step-independent solution is obtained. Both constant-volume and constant-pressure simulations are performed in the literature to calculate induction times for comparison with experimental shock tube data. A comparison of both approaches was performed by Schultz and Shepherd [34]. In case of stoichiometric undiluted hydrogen mixtures, the observed differences in induction time between constant-volume and constant-pressure simulations were smaller than 5%. In the limit of high dilution (this is the case in the present constant-pressure investigations) both induction times converged.

3.1. Results

Figure 1(a)–(f) shows a comparison of the numerically and experimentally obtained induction times for six pressures and equivalence ratios. The logarithmically scaled induction time is plotted versus the reciprocal temperature $1000/T$. At low pressures (0.45 bar in (a) and 0.43 bar in (b)) the differences between the investigated reaction mechanisms are marginal and the reproduction of the experimental results is quite good. The situation changes at higher pressures. Now the logarithmic induction time diagrams consist of two parts: a nearly linear increase at high temperatures (up to $1000/T = 0.85 - 0.95$) and a nonlinear section at lower temperatures. From these figures it becomes clear that the skeletal Jachimowski scheme (dotted line) is able to reproduce the ignition times at high temperatures very well but fails in predicting the increase in ignition delay at low temperatures. This is the price to be paid by neglecting HO_2 and H_2O_2 and the corresponding chemical reactions and reaction paths.

From Figure 1 it can also be seen that there are significant differences (orders of magnitude) between the detailed mechanisms at low temperatures. Unfortunately, this temperature range is relevant to scramjet combustors. The temperature at which the mechanisms start to diverge is shifted to higher values with increasing pressure. Moreover, there is also a large uncertainty in the experimental results at low temperatures, which may be seen by the scattering of the data. All investigated reaction mechanisms differ at least by one order of magnitude in comparison with the experiment for the 4 bar test case at temperatures below 1000 K (see Figure 1(f)). Similar differences are observed at 2 bar (see Figure 1(d)). For the 2.5 bar case no experimental low temperature data is available.

Induction times of the one-step kinetic model of Marinov *et al.* are included in the 1 bar plot of Figure 1(c) only, because this is the pressure the model is validated for. It can be observed that

DOI: 10.1002/fld

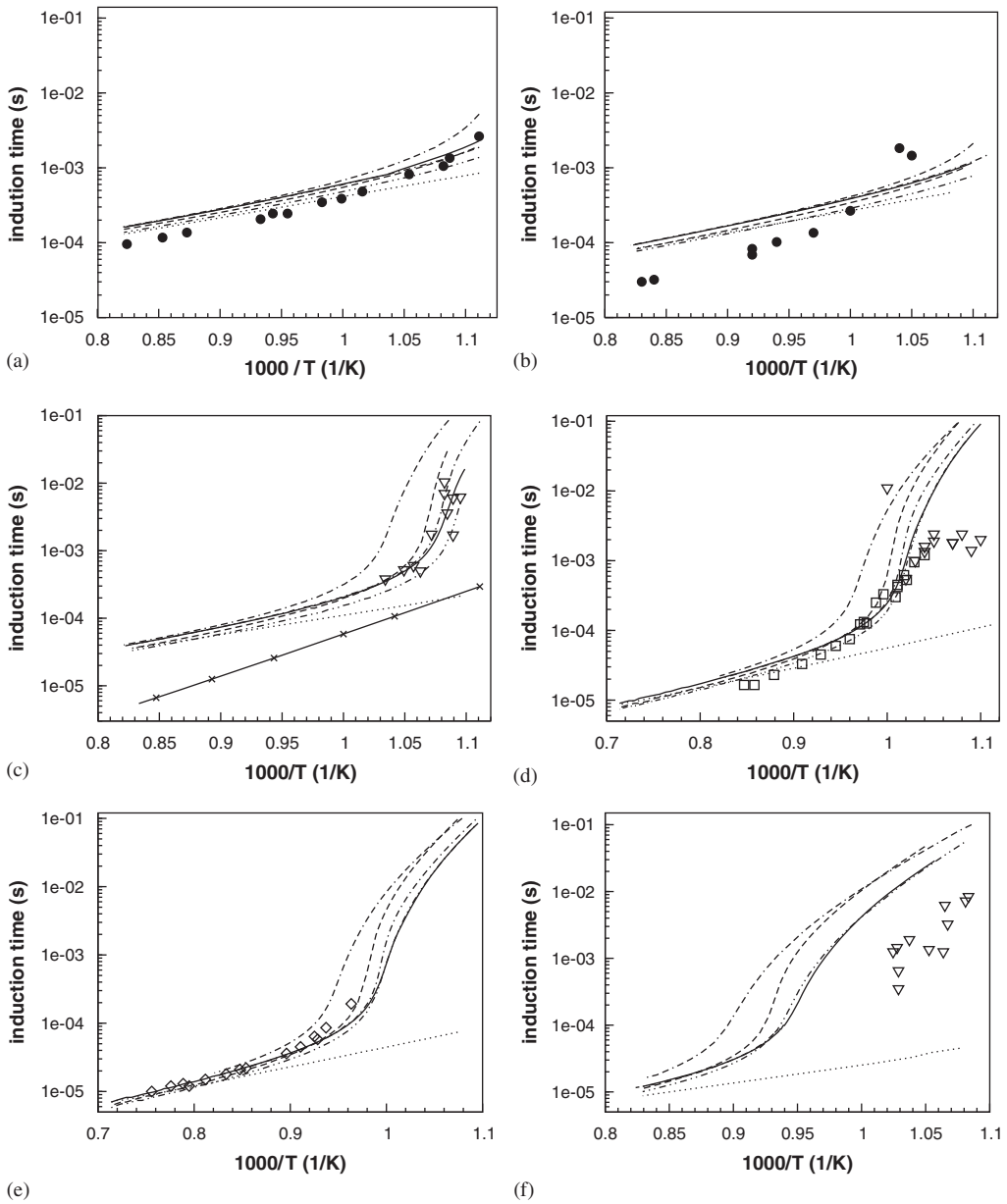

Figure 1. Comparison of induction times of diluted hydrogen/air mixtures at different pressures and equivalence ratios. Symbols are results from the experiments of: • Just and Schmalz [30], ▽ Sneyder *et al.* [31], □ Slack [32], ◊ Bhaskaran *et al.* [33]. Lines are results from simulations using the following reaction mechanisms: −·· Vajda *et al.* [5], −− Jachimowski [1], ··· skeletal Jachimowski [4], −·· Jachimowski [2], —— O'Conaire *et al.* [6], −−· GRI3.0 [7], ×——× Marinov *et al.* [8]: (a) $p=0.45$ bar, $\Phi=0.1$; (b) $p=0.43$ bar, $\Phi=1$; (c) $p=1$ bar, $\Phi=1$; (d) $p=2$ bar, $\Phi=1$; (e) $p=2.5$ bar, $\Phi=1$ and (f) $p=4$ bar, $\Phi=1$.

DOI: 10.1002/fld

the induction times are too short in comparison with the detailed mechanisms and the experiment. Even for higher temperatures the one-step reaction model is not able to reproduce the correct behaviour. Moreover, due to the lack of radicals the equilibrium temperatures are several hundred K to high. The results are similar for the other pressures. A reason for the discrepancies of the high-temperature induction times could be that the one-step model is validated to achieve correct laminar flame speeds that are connected to heat release.

Independent of pressure and equivalence ratio the principal behaviour of the investigated reaction mechanisms is the same for all six test cases. The skeletal Jachimowski scheme is the fastest one, followed by the Vajda *et al.* and the O'Conaire *et al.* mechanisms. Both Jachimowski mechanisms (1992 and 1988) are slightly slower. At all pressures the 1992 Jachimowski scheme is close to the O'Conaire *et al.* mechanism. Finally the GRI3.0 mechanism is significantly too slow (at low temperatures) in comparison with the experimental data. Similar results for the GRI3.0 mechanism have been observed by Ströhle and Myhrvold [26]. From Figure 1 it can be concluded that with the exception of the one-step kinetic model, the skeletal Jachimowski, and the GRI3.0 mechanism, the four remaining schemes are relatively close together and, at least at higher temperatures, are within the accuracy of the available experimental data. Especially for $\Phi = 1$ and $p = 1$ bar, they agree quite well with the experiment. This is important for the next test case, which is performed under atmospheric conditions.

4. TURBULENT SUPERSONIC COMBUSTION TEST CASE

Owing to the high effort required to achieve supersonic flames in ground test facilities, the number of experiments where the lift-off of the flame, temperature, and species profiles have been measured is rare (see, e.g., References [36–39]). Moreover most validation experiments are relatively old and there is some uncertainty concerning the accuracy of the measurement techniques, inflow, and boundary conditions. To the knowledge of the authors the Cheng *et al.* [36] experiment is the only one where the temperature and species have been measured simultaneously in high speed flows. This is important to assess the influence of turbulence chemistry interaction. Therefore this experiment is of special importance for supersonic combustion code validation. Even if the axisymmetric coflow configuration seems to be very simple, an accurate simulation of this lifted flame is quite demanding. The disadvantage of this and many other scramjet experiments is that the air inflow temperature is relatively high [40]. Hence, with respect to the reaction mechanism the inflow conditions are not the most critical ones that can appear in a scramjet combustor. On the other hand vitiated air is used that contains water from precombustion. According to Sung *et al.* [29] the ignition temperature for hydrogen/air mixtures with 20% water contamination (typical for scramjet experiments) is increased by about 100 K in comparison with dry air. This is due to the effectiveness of H_2O as a third body in recombination reactions. Thus, the water content increases the ignition delay and makes the experiment more critical to predict the correct point of ignition.

In the experiment of Cheng *et al.* [36] a pure hydrogen jet is injected at sonic speed into a vitiated supersonic (Ma = 2) coflow. The temperature of the hydrogen is 545 K and the temperature of the hot vitiated air (obtained by precombustion) is 1250 K. Figure 2 shows a sketch of the end of the precombustor, the air nozzle, and the hydrogen injector. The gas composition of the vitiated coflow is given by the following mass fractions: $Y_{O_2} = 0.245$, $Y_{N_2} = 0.58$, and $Y_{H_2O} = 0.175$. The experiment is performed at atmospheric pressure. The inner nozzle diameter (D) is 2.362 mm and all results shown will refer to non-dimensionalized positions normalized with this value. Under the

DOI: 10.1002/fld

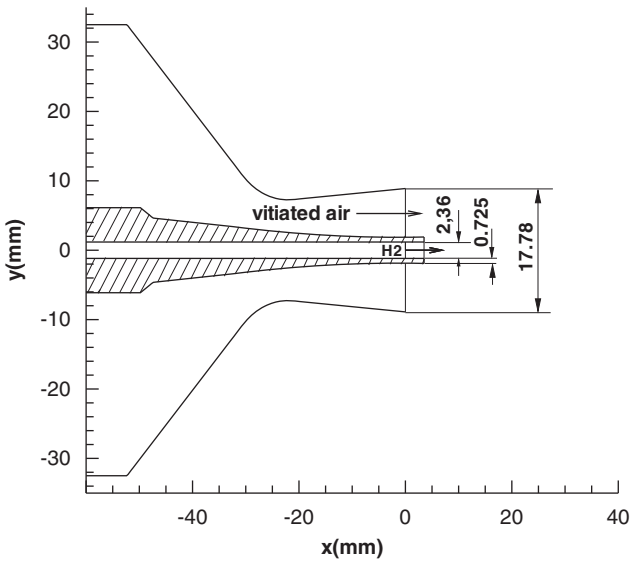

Figure 2. Setup of the Cheng *et al.* [36] experiment (dimensions in mm).

given conditions a lifted flame develops. The air temperature (1250 K) is relatively high and would correspond to scramjet flight Mach numbers of about 9. Owing to the previous investigation of induction times and based on the relatively high air temperature, the different reaction mechanisms should already be close together for this test case. However, the injected hydrogen (545 K) is significantly colder and the vitiated air has a high water content. Both effects increase the ignition delay time and shift the thermodynamic conditions closer to the self-ignition limit. Mean and root mean square (rms) values of velocities, temperature, major species H_2, O_2, N_2, H_2O, and the OH radical are available. It should also be mentioned that the experimental data were deteriorated by problems achieving axisymmetry, which is visible in some of the profiles.

4.1. Numerical simulation

Numerical simulations are performed using the in-house Turbulent All Speed Combustion Multigrid (TASCOM3D) solver [11, 41–44], which has been developed for the simulation of supersonic combustors. The full compressible Navier–Stokes, turbulence, species, and variance (of temperature and the sum of species mass fractions) transport equations are solved by an implicit Lower–Upper Symmetric Gauss–Seidel (LU-SGS) [45, 46] algorithm. The finite-volume scheme is second-order accurate in space. For turbulence closure a low-Reynolds number q–ω [47] ($q=\sqrt{k}$, k is the turbulent kinetic energy, $\omega=\varepsilon/k$, ε is the dissipation rate of k) model is used, which requires very fine grids near solid walls (all y^+ should be below 1). Local time stepping is used to accelerate convergence to a steady state. The steady-state solution is independent from the chosen time step. With respect to the different reaction mechanisms investigated, no differences in numerical stability have been observed. Stable, steady-state flames have been obtained with all mechanisms and with all computational grids under investigation. All simulations use a CFL number of 3. To account for turbulence–chemistry interaction a multi-variate assumed probability density

DOI: 10.1002/fld

function (PDF) approach is employed [43, 44, 48], assuming statistical independence between the species and temperature fluctuations. For the temperature a clipped Gaussian distribution is assumed and a transport equation for the temperature variance is solved. The joint PDF of an arbitrary number of species mass fractions is described by a multi-variate β-distribution [48], defined by the species mean mass fractions and the sum of species mass fraction variances, which are obtained from transport equations. The averaged chemical production rates may be calculated analytically with the assumed multi-variate β-distribution if the chemical reactions have integer stoichiometric coefficients. This is the case for all schemes based on elementary reactions (all detailed and skeletal mechanisms investigated). However, the one-step kinetic model of Marinov *et al.* [8] uses non-integer stoichiometric coefficients which is the reason why the assumed PDF closure may not be used. Thus, the simulation with the one-step kinetic is performed with 'laminar chemistry' only (source terms are calculated from mean values only). However, this does not affect the general evaluation of the model. The consideration of species and temperature fluctuations by the assumed PDF approach usually decreases the ignition delays of lifted flames. As will be shown later, the ignition length of the one-step kinetic model without turbulence–chemistry interaction is already much too short.

For a correct prediction of the lift-off height of the flame, the chosen reaction mechanism and the modeling of turbulence chemistry interaction are of great importance. Owing to the temperature differences between the hydrogen jet (545 K) and the surrounding air flow (1250 K) and the strong temperature sensitivity of many chain-initiating reactions, temperature fluctuations can play a significant role for an accurate calculation of the ignition delay. Further, due to the high velocities in scramjet combustors and the interaction of velocity and temperature, fluctuations of temperature and species concentrations are found to be higher than in subsonic flames [36]. Species and temperature fluctuations can be as high as 40 and 20%, respectively. The modeling approach used for turbulence–chemistry interaction has been investigated in several papers [43, 44], where the accuracy and the limits of the assumed multi-variate PDF model have been studied. The overall agreement with experimental data was quite good. Additionally, a transported joint scalar–velocity–frequency Monte-Carlo PDF simulation was performed [49]. The transported PDF approach is physically more sound, but for complex three-dimensional simulations the multi-variate assumed PDF method is used by the authors due to its higher numerical efficiency. Moreover, methods for convergence acceleration [11] and a good shock capturing are reasons for employing a conventional finite-volume method with assumed PDF closure.

4.2. Inflow conditions and grid sensitivity

The Cheng *et al.* [36] experiment has been used by numerous authors for code validation [9, 17, 43, 44, 49–51]. All cited simulations neglect OH and other radicals in the vitiated air stream that are due to preburning. However, in the experiment traces of OH ($X_{OH} \approx 0.001$) have been observed in the initial plane of measurement still upstream of the point of ignition. Cheng *et al.* [36] concluded that chemical equilibrium is reached in the precombustor and that the composition remains unchanged during acceleration in the nozzle. As it is shown later, radicals from preburning have a significant influence on the ignition delay. However, a first series of simulations is performed without the consideration of radicals. Figure 3 shows temperature plots of these simulations using seven different reaction mechanisms. The computational grid consists of five blocks that extend into the interior of the inner and outer injector tubes. The grid has 332×36, 296×36, 344×120, 328×16, and 344×66 volumes (in total 91 840 volumes). It is strongly refined in all near wall

DOI: 10.1002/fld

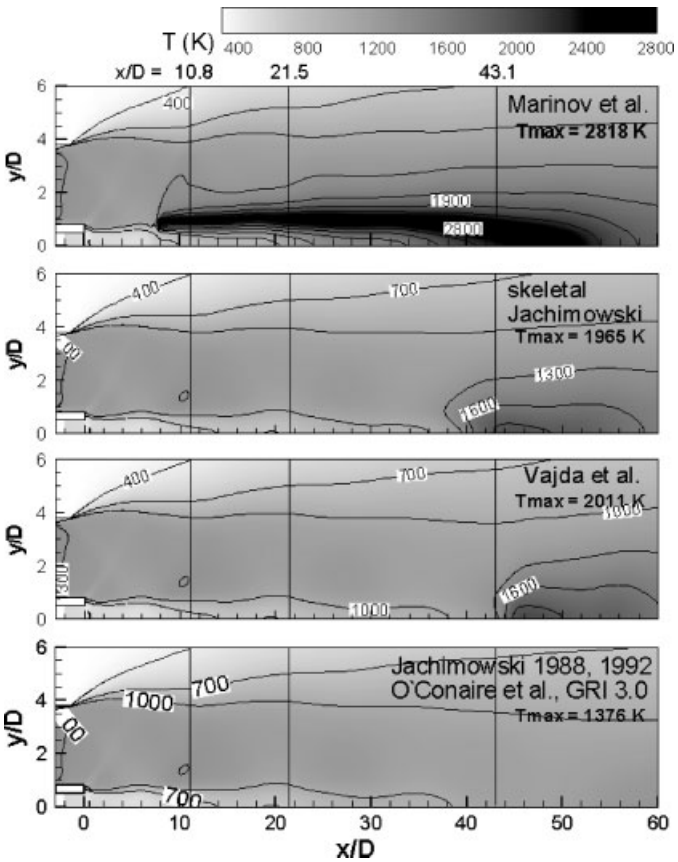

Figure 3. Calculated mean temperature distributions for the Cheng *et al.* [36] experiment using different reaction mechanisms without radicals in the vitiated air stream (ΔT between isolines is 300 K).

regions and in the ignition and the combustion zones. The solution was found to be grid independent on this grid. The distance from the near wall cell centres to the solid wall is approximately $1.3 \cdot 10^{-6}$ m. Precalculated, fully turbulent inlet profiles are used for the hydrogen and the vitiated air. All simulations have been initialized with identical cold flow fields. As can be seen from Figure 3, strong differences are obtained by changing the reaction scheme ($x/D = 0$ corresponds to the nozzle exit and $y/D = 0$ to the symmetry line). The reason is that the thermodynamic conditions are close to the ignition limit of the hydrogen/air mixtures. Despite the fact that turbulent fluctuations play an additional role, the same behaviour as before in the zero-dimensional investigation is observed: the one-step scheme of Marinov *et al.* has the shortest ignition delay, followed by the skeletal Jachimowski scheme and the Vajda *et al.* mechanism. The reaction schemes of O'Conaire *et al.*, the 1988 and 1992 Jachimowski schemes, and the GRI3.0 mechanism do not ignite at all. Even the skeletal Jachimowski scheme and the Vajda *et al.* mechanism are close to a blow-off of the flame. In these cases the lift-off height is significantly longer than in the experiment, where ignition occurs between the axial locations $x/D \approx 18$ and $x/D = 25$. Asymmetry was observed in

DOI: 10.1002/fld

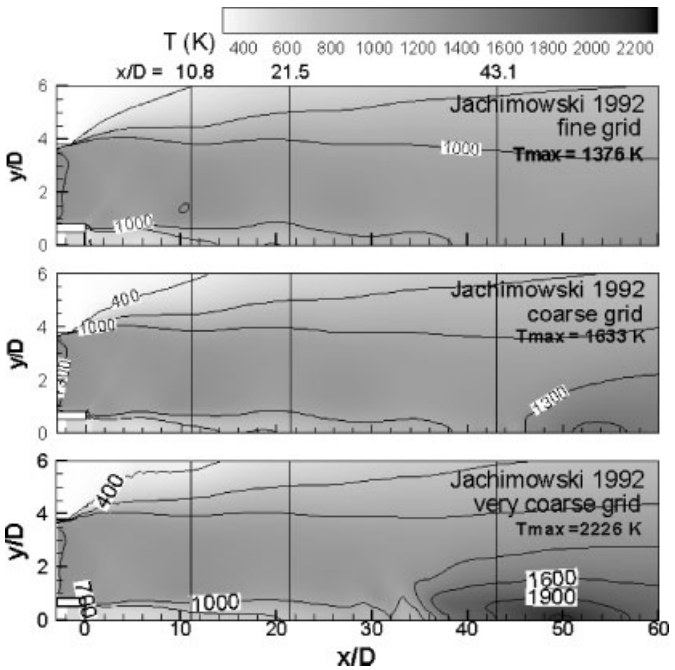

Figure 4. Calculated mean temperature distributions for the Cheng *et al.* [36] experiment without radicals in the vitiated air stream (ΔT between isolines is 300 K). The three pictures correspond to simulations using different grids (91 840 volumes top, 22 960 volumes middle, 11 480 volumes bottom).

the experiment in radial direction and the temperature profiles at $x/D = 21.5$ indicate that at one side of the jet there already is combustion (see later Figure 13).

It can be summarized that the one-step mechanism achieves an ignition delay that is much too short and therefore should not be used for the simulation of lifted flames. Moreover, the temperature level in the combustion zone is about 400 K too high due to neglected radicals, making its use even more questionable. All remaining reaction mechanisms cause ignition delays that are significantly too long compared with the experiment and the flame structures and temperature profiles do not agree with the experimental data. Thus the question arises why previous simulations, which also neglected radicals in the inflow, achieved much better results. The reason is the computational grid, which was much too coarse in all cases. If the 1992 Jachimowski mechanism is used, no ignition takes place on a sufficiently fine computational grid. If the same simulation is performed on coarser grids, ignition takes place and, in some cases, results agree quite well with the experiment. Figure 4 shows the temperature contours using the 1992 Jachimowski mechanism on different grids. The fine grid is the grid described before, while the coarse grid neglects every second grid point in both the coordinate directions, and the very coarse grid neglects every second grid point of the coarse grid in the axial direction. The figures show that ignition is moving upstream with decreasing grid size. This is in agreement with implicit first-order zero-dimensional simulations of an adiabatic stoichiometric PSR. Figure 5 shows the corresponding temperature plots for an initial temperature of 1200 K and a pressure of 1 bar, respectively. Simulations are performed with time steps ranging from $1 \cdot 10^{-8}$ s to $2.4 \cdot 10^{-6}$. A first-order Euler implicit scheme is used for time

DOI: 10.1002/fld

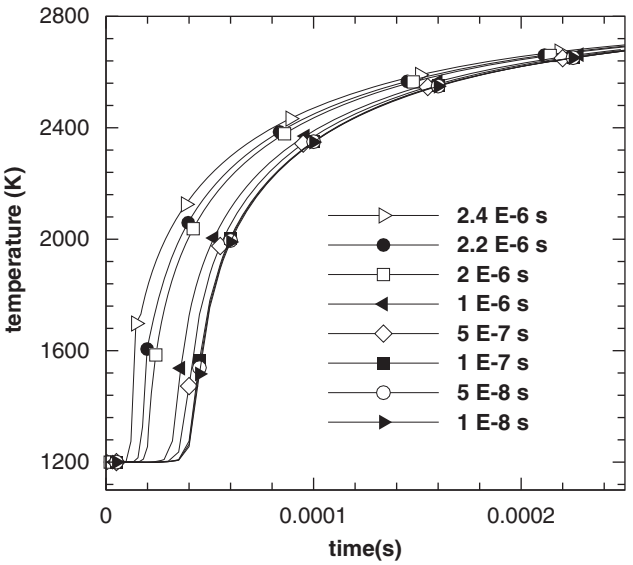

Figure 5. Influence of the chosen time step Δt (s) on the ignition delay of a stoichiometric hydrogen air mixture at 1 bar constant pressure (1992 Jachimowski [2] mechanism).

integration. The last three temperature profiles ($\Delta t \leqslant 1 \cdot 10^{-7}$ s) collapse into 1 line and reach a time step-independent solution. If the time step is too large, the ignition delay is too short (the ignition delay decreases with increasing time step size). The reason is the exponential growing of radicals in the ignition delay zone (or lift-off region) by many orders in magnitude that has to be accurately resolved in time (or in space in the case of lifted flames). Figure 6 shows OH and H_2O_2 mass fraction profiles for simulations with time steps of $2 \cdot 10^{-6}$ s and $1 \cdot 10^{-8}$ s. The exponential increase of these species is representative of the other radicals (H, HO_2, and H_2O_2). A simple investigation of the monotonically increasing model function $dy/dt = e^t$ $(y(t=0)=0)$ shows that a first-order Euler implicit time integration

$$y^{n+1} = y^n + \Delta t e^{n+1} \tag{1}$$

overpredicts the increase in y (due to the use of the higher-value e^{n+1}), while a first-order explicit time integration

$$y^{n+1} = y^n + \Delta t e^n \tag{2}$$

causes an underprediction (because the lower value e^n is used). A first-order upwind discretization of a spatially one-dimensional steady-state problem corresponds to Equation (1) and thus causes a reduction of the ignition delay, if the computational grid is not fine enough. For the model equation it can be shown easily that a spatially second-order upwind discretization for the same problem reduces the error term to second order, but it still causes a reduction in lift-off length (if the computational grid is not fine enough). The two-dimensional simulations of the Cheng *et al.* experiment are second order in space, but due to total variation diminishing (TVD) flux limitations at the shock waves downstream of the injector the order locally may be reduced. At shock waves

DOI: 10.1002/fld

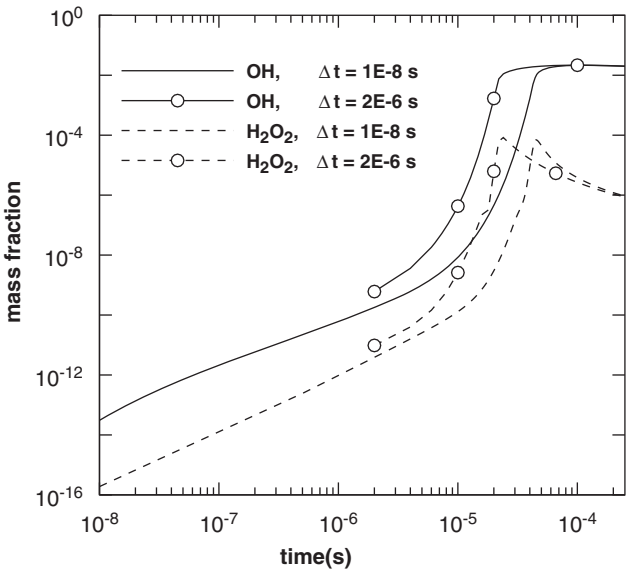

Figure 6. Influence of the chosen time step Δt (s) on the formation of OH and H_2O_2 in a stoichiometric hydrogen air mixture at 1 bar constant pressure (1992 Jachimowski [2] mechanism).

TVD limiters adapt the numerical scheme to become first-order upwind, which increases the underprediction of the ignition delay.

Therefore, it can be concluded that the grid spacing has to be very fine in the lift-off region of the flame to achieve a correct lift-off height. This problem has probably been underestimated in the past.

4.3. Precombustor nozzle flow

Next, the influence of radicals from precombustion is investigated. In the previous section it has been observed that no ignition takes place for some reaction schemes if radicals are neglected at the inlet. Because OH has been measured at the precombustor exit on one side of the radial profile only (for $y/D \geqslant 0$) [36], there is some uncertainty in this value. Therefore, a separate reactive flow simulation has been performed for the precombustor nozzle to obtain more accurate inflow conditions for the subsequent supersonic flame calculation. In the precombustor chemical equilibrium is assumed. According to Jarrett *et al.* [50] the nozzle exit area is known quite accurately, while the throat area is sensitive to manufacturing tolerances. Therefore the simulation uses the given exit area, while the throat area is determined according to the measured mass fluxes. An attempt was made to obtain a good agreement between the measured and simulated mass fluxes and the combustor total pressure. These values are known quite well and have been measured within $\pm 4\%$ accuracy. Table III summarizes the corresponding experimental and numerical values. The nozzle exit temperature has also been measured, but all remaining experimental values are evaluated or obtained by one-dimensional, isentropic, frozen equilibrium analysis [50]. With the exception of the total temperature in the precombustor all values are in good agreement. For the total temperature a higher value is used in the simulation ($T_t = 1920\,\mathrm{K}$), which was needed to

DOI: 10.1002/fld

Table III. Comparison of experimental and numerical preburner conditions.

	Experiment [36]	Simulation
Vitiated air mass flow rate (kg/s)	0.09633 (±2.2%)	0.0944
Fuel (H_2) mass flow rate (kg/s)	0.000362 (±3%)	0.0003502
Total pressure (bar)	7.78 (±4%)	7.66
Total temperature (K)	1750	1920
Exit pressure (bar)	1.07	1.15*
Exit temperature (K)	1250	1280*
Exit Mach number	2.0	1.9*

*Numerical values are at the end of the outer tube; experimental ones at the end of the inner tube that is 3.5 mm further downstream.

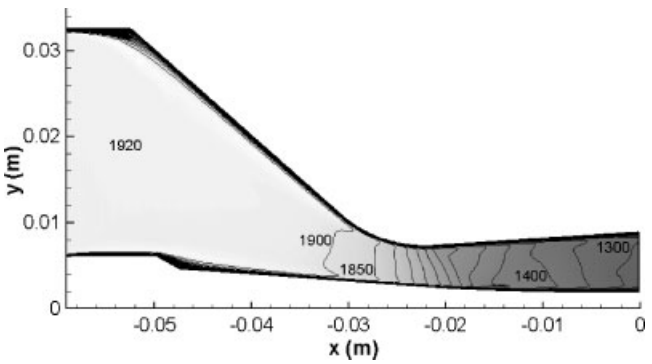

Figure 7. Calculated temperature distribution in the preburner nozzle using the 1988 Jachimowski [1] mechanism.

obtain the measured exit temperature of 1250 K. Because the mass fluxes also agree very well, we believe our value to be the correct one. The precombustor simulation is performed using the assumed PDF approach and the 1988 Jachimowski reaction mechanism. A wall temperature of 570 K is assumed, which is evaluated from the measured hydrogen injection temperature of 550 K. The computational grid consists of 300 volumes in the axial and 80 in the radial directions. Figures 7 and 8 show the calculated temperature and OH distributions in the preburner nozzle. From this simulation inlet profiles are extracted for the following supersonic flame calculations. Because the computational grid extends into the interior of the inner and outer tubes, profiles are taken at $x = -3.5$ mm. At this position the molar fractions of OH, O, and H in the main flow are $0.9313 \cdot 10^{-3}$, $0.1686 \cdot 10^{-3}$, and $0.1789 \cdot 10^{-4}$, respectively. These values decrease near the cooled upper and lower walls as may be seen from the OH distribution given in Figure 8. The calculated OH molar fraction compares quite well with the experimentally measured value of $X_{OH} \approx 0.001$.

4.4. Results and discussion

The following supersonic flame simulations use inlet profiles from the precombustor simulation and thus take radicals from precombustion into account. The calculations are performed on the

DOI: 10.1002/fld

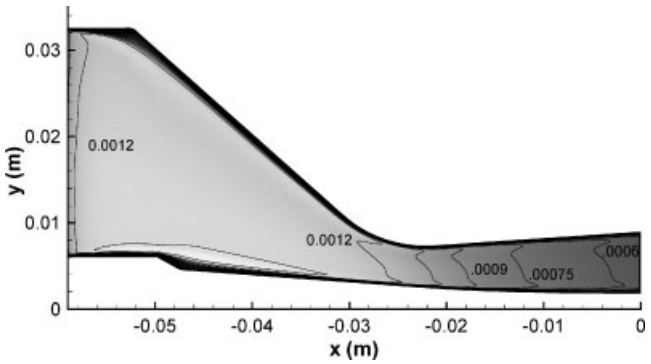

Figure 8. Calculated OH mass fraction distribution in the preburner nozzle using the 1988 Jachimowski [1] mechanism.

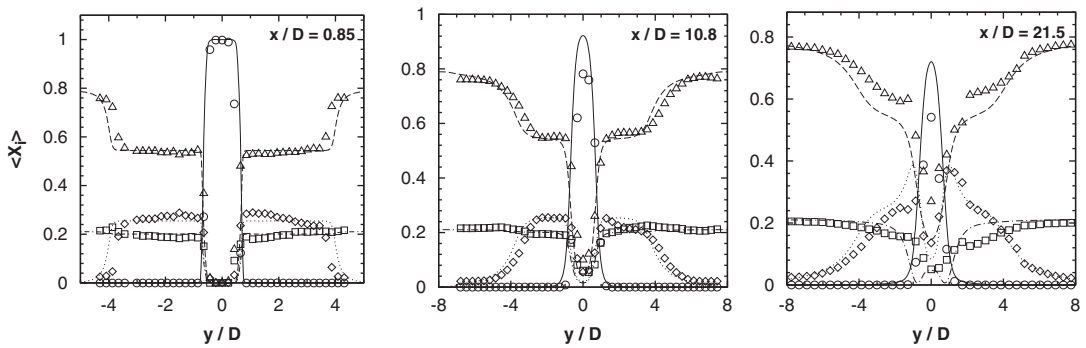

Figure 9. Comparison of experimental and numerical molar fraction profiles at the positions $x/D=0.85, 10.8$, and 21.5 using the 1992 Jachimowski [2] mechanism. Symbols are results from the experiment: $\circ H_2$, $\triangle N_2$, $\square O_2$, $\Diamond H_2O$. Lines are results from the simulation: —— H_2, $- - N_2$, $\cdot - \cdot O_2$, $\cdots H_2O$.

same 5 block grid (in total 91 840 volumes) as before. For comparison, an additional simulation has been performed on a further refined grid with 183 680 volumes (about 680 volumes in axial and 270 volumes in radial direction). No influence on the ignition delay was observed and there was only a negligible influence on the species and temperature profiles. Therefore the 5 block grid with 91 840 volumes is used in the following study.

To demonstrate the ability of the code to accurately describe the mixing process upstream of the point of ignition, Figure 9 shows H_2, N_2, O_2, and H_2O profiles for $x/D=0.85, 10.8$, and 21.5 using the 1992 Jachimowski mechanism. The first two positions are still upstream of the point of ignition and therefore independent of the kinetic scheme used. The overall agreement with the experiment is quite good. At the third position (at $x/D=21.5$), there already is combustion and differences are caused by the kinetic scheme too, as discussed in more detail later. Figure 10 shows the calculated pressure distribution for the region around the injector up to the position where ignition takes place ($x\approx 0.05$ m). A system of shock waves and expansion fans can be observed,

DOI: 10.1002/fld

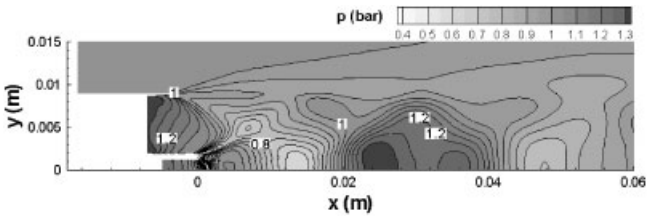

Figure 10. Calculated pressure distribution (bar) near the nozzle exit using the 1992 Jachimowski [2] mechanism.

which further downstream disappears quickly. Especially in the region where combustion takes place ($x>0.045$ m), the changes in pressure are relatively small. Thus, the direct impact of changes in pressure on the rate constants of the pressure-dependent reactions (of the O'Conaire *et al.* or the GRI mechanism) is negligible. However, there is an effect of local pressure gradients on the chemical reaction rates due to changes in species concentrations.

4.4.1. Ignition delay. Figures 11 and 12 show temperature and OH molar fraction contours, respectively. In contrast to the previous simulations, ignition now takes place with any reaction mechanism investigated. This demonstrates the need to consider radicals from precombustion in the inflow. In addition, it may explain the asymmetry observed in the experiment in the radial direction (see, e.g., the temperature profile at $x/D=21.5$ plotted in Figure 13). At this position ignition has already taken place for $y/D\geqslant 0$. This is the same part of the profile where OH has been measured at the inlet. For $y/D\leqslant 0$, the inlet OH concentration has been below the detection limit of $X_{OH}\approx 0.0003$ [36] and ignition takes place further downstream. Owing to the strong dependency of the ignition length from the OH inflow value, the asymmetric OH distribution measured at the precombustor outlet [36] is the most likely reason for the asymmetries observed in the flame. However, a point against this assumption is that at $x/D=10.8$ (see Figure 14) the experimental OH profile is symmetric while further downstream it is not. Because the present simulation uses inflow conditions that correspond to $y/D>0$ in the experiment, the corresponding values should be taken for comparison.

For this experiment the differences caused by the assumed PDF approach are relatively small. All results shown here are obtained using the described assumed PDF closure (a Gaussian distribution for temperature and a multi-variate β-distribution for the species mass fractions). Simulations without it ('laminar chemistry') resulted in slightly shifted points of ignition only. The maximum temperatures without PDF closure are smaller (2045 K instead of 2238 K for the 1988 Jachimowski mechanism, and 2175 K instead of 2247 K for the O'Conaire *et al.* scheme), and the maximum OH concentrations are higher (about 20%). Overall the differences are relatively small, but the assumed PDF approach improves the results when compared with the experiment.

Owing to the radicals from precombustion the chemical and thermodynamic conditions for ignition are much less critical than before, and the results using the different kinetic schemes are quite close together. However, the Vajda *et al.* mechanism again causes ignition too early and the GRI3.0 mechanism too late. The remaining mechanisms only differ slightly in their temperature and OH distributions as well as in their maximum values. The skeletal and the detailed

DOI: 10.1002/fld

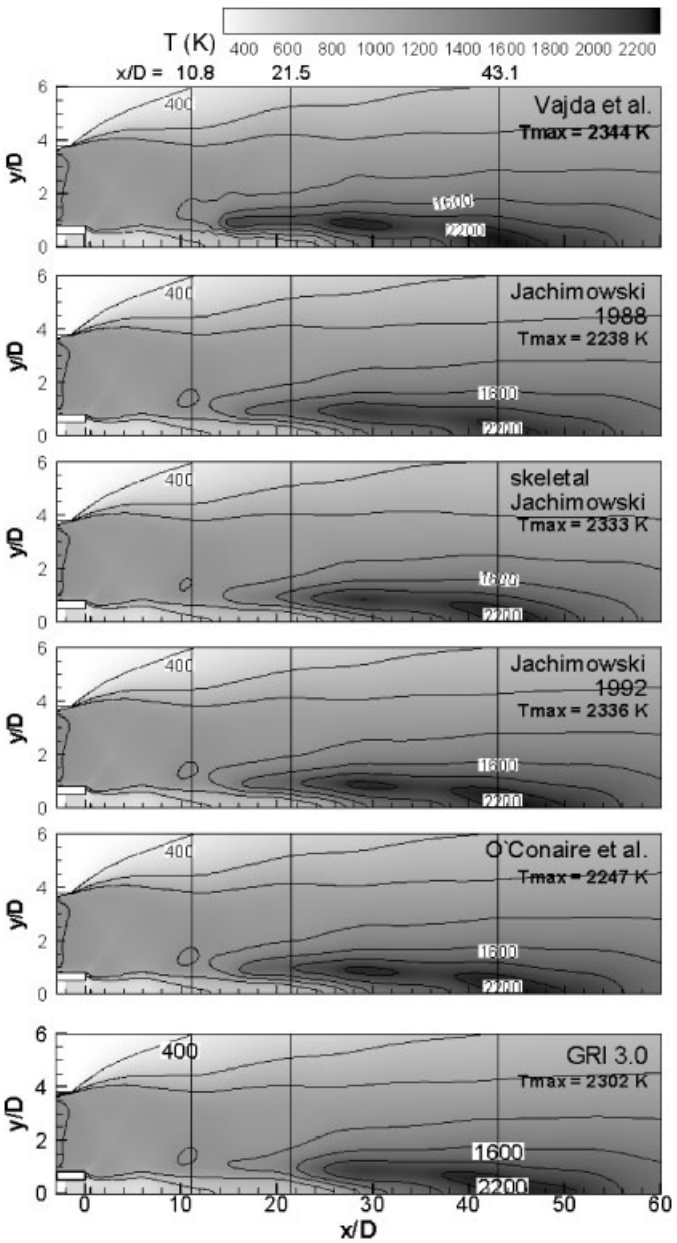

Figure 11. Calculated mean temperature distributions for the Cheng *et al.* [36] experiment using different reaction mechanisms (ΔT between isolines is 300 K).

DOI: 10.1002/fld

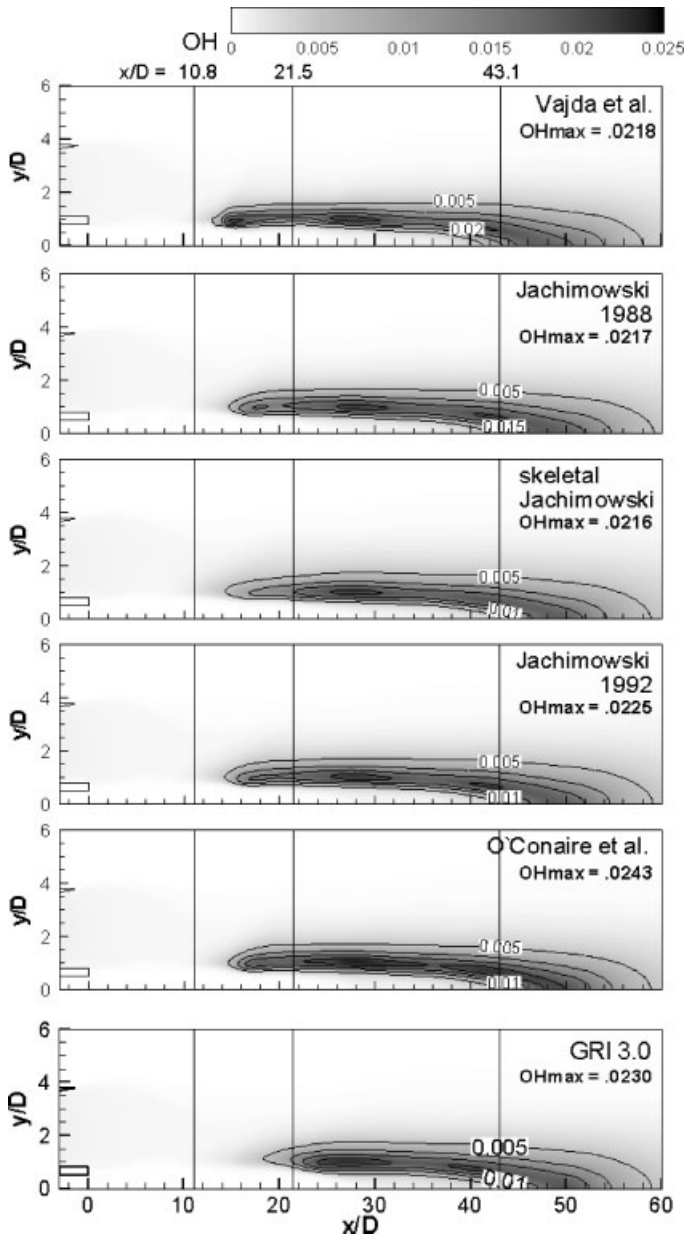

Figure 12. Calculated mean OH molar fraction distributions for the Cheng *et al.* [36] experiment using different reaction mechanisms (ΔX_{OH} between isolines is 0.005).

1988 Jachimowski schemes agree quite well concerning their ignition delays, but differ in the maximum temperature by about 100 K. This comparison shows that the skeletal scheme can be used with small losses in accuracy only, if the conditions are not close to the ignition limit of the

DOI: 10.1002/fld

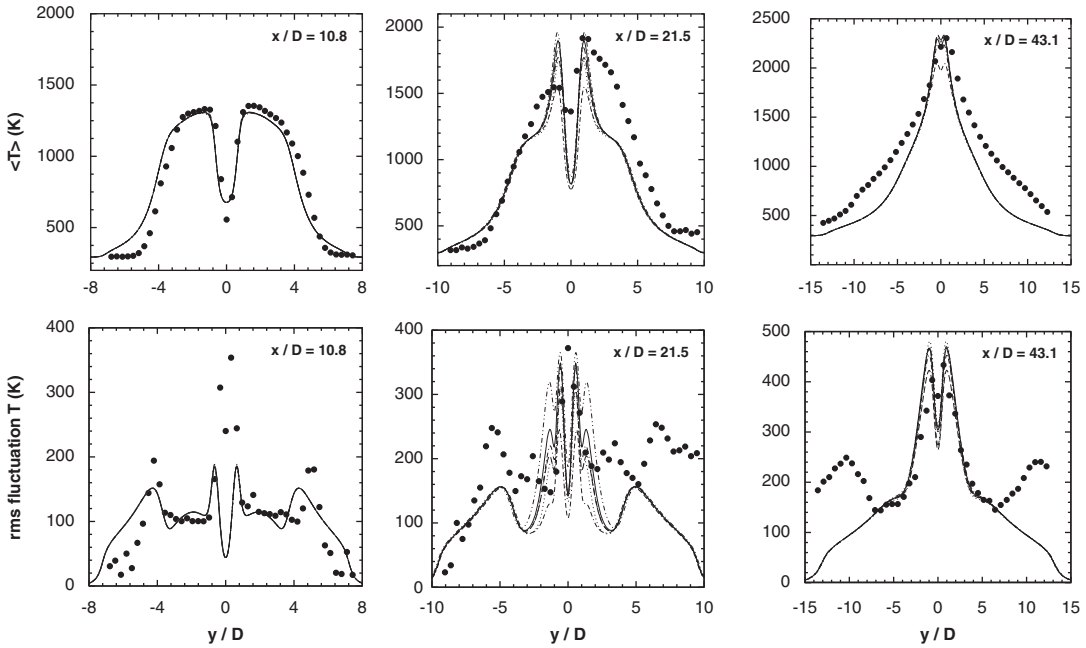

Figure 13. Comparison of mean temperature (upper line) and rms temperature fluctuation (lower line) profiles at three positions downstream of the injector. Symbols (•) are results from the experiment of Cheng *et al.* [36], lines are results from simulations using the following reaction mechanisms: −·· Vajda *et al.* [5], − Jachimowski [1], ··· skeletal Jachimowski [4], ·−· Jachimowski [2], —— O'Conaire *et al.* [6], −−· GRI3.0 [7].

fuel–air mixture. This is in contrast to the one-step scheme that yields bad results even under those conditions.

4.4.2. Temperature and species profiles. Radial profiles (mean and rms values) of temperature and species molar fractions (of OH and H_2O) are compared with the experimental data in Figures 13, 14 and 15. The rms values of species molar fractions are calculated from the multi-variate β-distribution using the local mean species mass fractions (first moments) and the sum of the species mass fraction fluctuations (second moment). The rms value of temperature is obtained directly by solving a corresponding transport equation. The axial positions of the radial profiles are at $x/D = 10.8, 21.5$, and 43.1 and are marked in the contour plots of Figures 11 and 12 by the vertical lines. The upper three plots in any figure show the mean values at the positions mentioned, whereas the lower three figures the corresponding rms values. Profiles of the one-step kinetic scheme are not included, because both temperature (by several hundred K) and species molar fractions (up to 40%) are highly erroneous.

With the exception of the profile using the Vajda *et al.* and the GRI3.0 mechanisms, all mean values are close together and agree well with the experimental data. At the first position shown at $x/D = 10.8$ (this is still upstream of the point of ignition), the experimental OH molar fraction has already increased from 0.001 at the inlet up to ≈ 0.0018. This behaviour is only reproduced by the skeletal Jachimowski scheme. Further downstream the mean OH profiles are quite well

DOI: 10.1002/fld

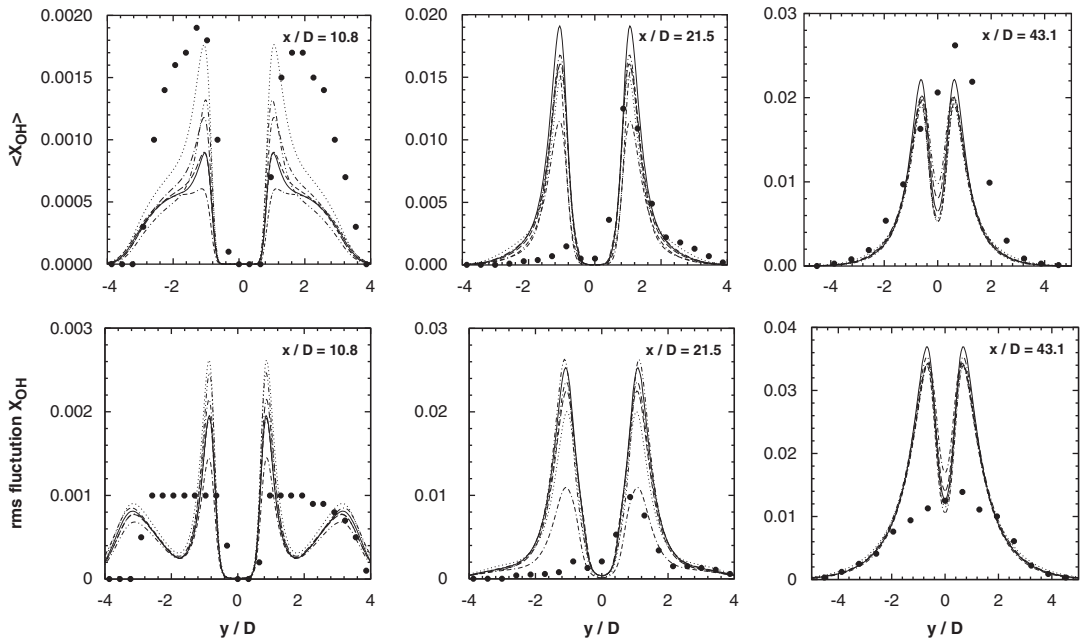

Figure 14. Comparison of mean OH molar fraction (upper line) and rms OH molar fraction fluctuation (lower line) profiles at three positions downstream of the injector. Symbols (•) are results from the experiment of Cheng *et al.* [36], lines are results from simulations using the following reaction mechanisms: −·· Vajda *et al.* [5], −− Jachimowski [1], ··· skeletal Jachimowski [4], ·−· Jachimowski [2], —— O'Conaire *et al.* [6], −−· GRI3.0 [7].

predicted by the simulations. Concerning the rms values, temperature and water profiles agree quite well with the experiment, while there are discrepancies in the OH rms values. The simulated OH fluctuations at $x/D=21.5$ and 43.1 are at least by a factor of two higher than in the experiment. This is probably due to the relatively simple assumed PDF approach.

5. CONCLUSIONS

A validation experiment for supersonic combustion has been investigated with respect to reaction mechanism, grid spacing, and inflow conditions. At low flight Mach numbers of a scramjet, the thermodynamic conditions are close to the self-ignition limit of hydrogen/air mixtures. Under such conditions lifted flames react sensitively to changes of all the investigated parameters. Some of the most frequently used reaction mechanisms in supersonic combustion have been tested. It has been shown that at $1000/T>0.95$ and $p\approx 1$ bar

- detailed kinetic schemes have to be used (both the skeletal and the one-step kinetic scheme are highly erroneous) and
- large differences (one order of magnitude and more) in ignition delay are obtained between the detailed mechanisms investigated.

DOI: 10.1002/fld

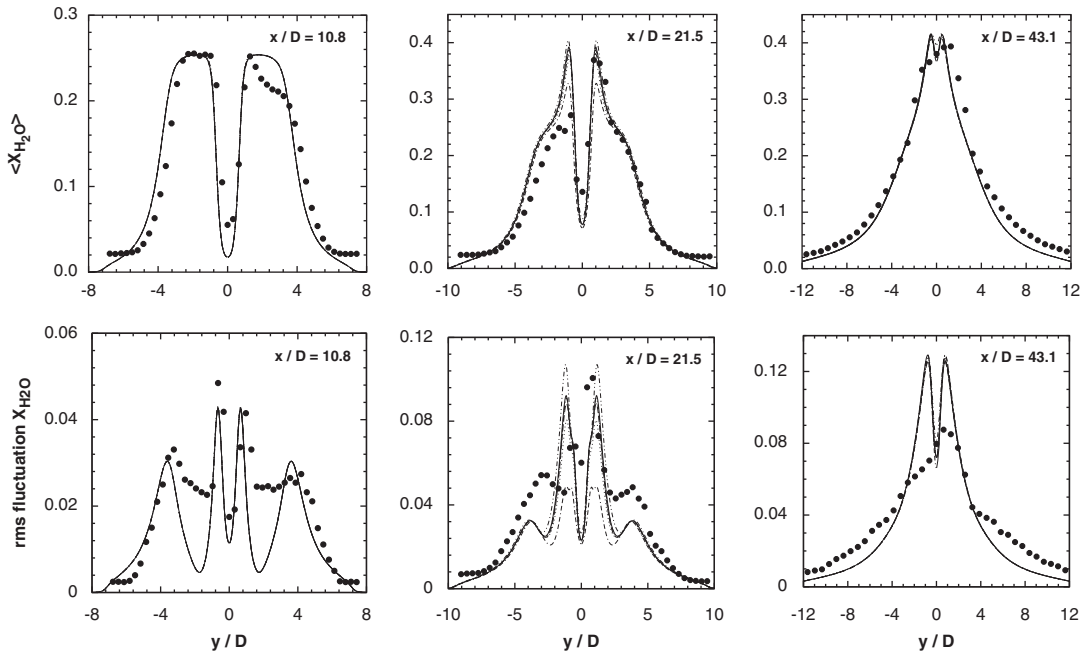

Figure 15. Comparison of mean H_2O molar fraction (upper line) and rms H_2O molar fraction fluctuation (lower line) profiles at three positions downstream of the injector. Symbols (•) are results from the experiment of Cheng *et al.* [36], lines are results from simulations using the following reaction mechanisms: $-\cdot\cdot$ Vajda *et al.* [5], $-$ Jachimowski 1988 [1], $\cdots$ skeletal Jachimowski [4], $\cdot-\cdot$ Jachimowski [2], —— O'Conaire *et al.* [6], $--\cdot$ GRI3.0 [7].

The one-step kinetic scheme was found to be inappropriate due to wrong ignition delays and temperatures even under less critical conditions. This is in contrast to the skeletal Jachimowski scheme that can be used if the temperature in the combustor is high enough ($1000/T < 0.95$ for $p \approx 1$ bar). Concerning the detailed mechanisms investigated

- the Vajda *et al.* mechanism was found to be too fast and
- the GRI3.0 mechanism to be too slow

in comparison with the experiment. The best results are obtained with the O'Conaire *et al.* and the 1992 Jachimowski mechanisms. Surprisingly, the 1992 Jachimowski mechanism performed somewhat better than the 1988 version, which is mostly found in the literature. Concerning the simulation of lifted flames, very fine grids have to be used in the lift-off region to correctly recover the increase in the radical concentrations (by several orders in magnitude) and to obtain a correct lift-off length. This problem has been underestimated by many researchers in the past. It has been shown that an exceedingly coarse computational grid causes a reduction in the ignition delay if an upwind scheme is used. For the Cheng *et al.* [36] experiment, which is one of the most important test cases for supersonic combustion code validation, the consideration of radicals from precombustion is mandatory. Probably this is also the case for most other supersonic combustion experiments using precombustion.

DOI: 10.1002/fld

ACKNOWLEDGEMENTS

Parts of this work have been performed within the Long-Term Advanced Propulsion Concepts and Technologies (LAPCAT) project investigating high-speed air-breathing propulsion. LAPCAT, coordinated by ESA-ESTEC, is supported by the EU within the Sixth Framework Programme Priority 1.4, Aeronautic and Space, contract no.: AST4-CT-2005-012282. Further info on LAPCAT can be found on http://www.esa.int/techresources/lapcat.

We would like to thank the Höchstleistungsrechenzentrum Stuttgart (HLRS) and the Deutsche Forschungsgemeinschaft (DFG) for the provision of computational resources.

We also wish to thank Prof. T. S. Cheng and Prof. R. W. Pitz for providing experimental data in electronic form.

REFERENCES

1. Jachimowski CJ. An analytical study of the hydrogen–air reaction mechanism with application to scramjet combustion. *NASA-TP-2791*, 1988.
2. Jachimowski CJ. An analysis of combustion studies in shock expansion tunnels and reflected shock tunnels. *NASA-TP-3224*, 1992.
3. Wilson GJ, MacCormack RW. Modeling supersonic combustion using a fully implicit numerical method. *AIAA Journal* 1992; **30**:1008–1015.
4. Gaffney RL, White JA, Girimaji SS, Drummond JP. Modeling turbulent/chemistry interactions using assumed PDF methods. *AIAA Paper 92-3638*, 1992.
5. Vajda S, Rabitz H, Yetter RA. Effects of thermal coupling and diffusion on the mechanism of H_2 oxidation in steady premixed laminar flames. *Combustion and Flame* 1990; **82**:270–292.
6. O'Conaire M, Curran HJ, Simmie JM, Pitz RW, Westbrook CG. A comprehensive modeling study of hydrogen oxidation. *International Journal of Chemical Kinetics* 2004; **11**:602–622.
7. Smith GP, Golden DM, Frenklach M, Moriarty NW, Eiteneer B, Goldenberg M, Bowman CT, Hanson RK, Song S, Gardiner WC, Lissianski VV, Qin Z. GRI3.0 mechanism, 1995. Available from: http://www.me.berkeley.edu/gri_mech/.
8. Marinov NM, Westbrook CK, Pitz WJ. Detailed and global chemical kinetics model for hydrogen. In *Proceedings of the Eighth International Symposium on Transport Phenomena in Combustion*, Chan SH (ed.). Taylor & Francis: London, 1995; 118–129.
9. Baurle RA, Alexopoulos GA, Hassan HA. Modeling of supersonic turbulent combustion using assumed probability density functions. *Journal of Propulsion and Power* 1994; **10**:777–786.
10. Ali M, Fujiwara T, Leblanc JE. Influence of main flow inlet configuration on mixing and flameholding in transverse injection into supersonic airstream. *International Journal of Engineering Science* 2000; **38**:1161–1180.
11. Gerlinger P, Möbus H, Brüggemann D. An implicit multigrid method for turbulent combustion. *Journal of Computational Physics* 2001; **167**:247–276.
12. Kim JH, Yoon Y, Jeung IS, Huh H, Choi JY. Numerical study of mixing enhancement by shock waves in model scramjet engines. *AIAA Journal* 2003; **41**:1074–1080.
13. Dessornes O, Scherrer D. Tests of the JAPHAR dual mode Ramjet engine. *Aerospace Science and Technology* 2005; **9**:211–221.
14. Calhoon WH, Brinckman KW, Tomes J, Mattick SJ, Dash M. Scalar fluctuation and transport modeling application to high speed reacting flows. *AIAA Paper 2006-1452*, 2006.
15. Narayan JR. Two-equation turbulence model for compressible reacting flows. *AIAA Journal* 1993; **31**:398–400.
16. Baurle RA, Alexopoulos GA, Hassan HA. Assumed joint probability density function approach for supersonic turbulent combustion. *Journal of Propulsion and Power* 1994; **10**:473–484.
17. Baurle RA, Girimaji SS. Assumed PDF turbulence–chemistry closure with temperature–composition correlations. *Combustion and Flame* 2003; **134**:131–148.
18. Keistler PG, Gaffney RL, Xiao X, Hassan HA. Turbulence modeling for scramjet applications. *AIAA Paper 2005-5382*, 2005.
19. Tsuboi N, Katoh S, Hayashi AK. Three dimensional numerical simulation for hydrogen/air detonation: rectangular and diagonal structures. *Proceedings of the Combustion Institute* 2002; **29**:2783–2788.
20. Mueller MA, Yetter RA, Dreyer FL. Flow reactor studies and kinetic modeling of the H_2/O_2 reaction. *International Journal of Chemical Kinetics* 1999; **31**:113–125.

DOI: 10.1002/fld

21. Chen JH, Hawkes ER, Sankaran R, Mason SD, IM HG. Direct numerical simulation of ignition front propagation in a constant volume with temperature inhomogeneities. I. Fundamental analysis and diagnostics. *Combustion and Flame* 2006; **145**:128–144.
22. Sreedhara S, Huh KY. Assessment of closure schemes in second-order conditional moment closure against DNS with extinction and ignition. *Combustion and Flame* 2005; **143**:386–401.
23. Bastiaans RJ, Vreman AW, Pitsch H. DNS of lean hydrogen combustion with flamelet-generated manifolds. Center of Turbulence Research, Annual Research Briefs, 2007. Available from: http://www.stanford.edu/group/ctr/publications.html.
24. Li L, Zhao Z, Kazakov A, Dryer FL. An updated comprehensive kinetic model of hydrogen combustion. *International Journal of Chemical Kinetics* 1999; **36**:566–575.
25. San Diego mechanism 2005/10/11, 2005. Available from: http://maemail.ucsd.edu/combustion/cermech/.
26. Ströhle J, Myhrvold T. An evaluation of detailed reaction mechanisms of hydrogen combustion under gas turbine conditions. *International Journal of Hydrogen Energy* 2007; **32**:125–135.
27. Choi JY, Yang VY, Ma F, Wong SH, Jeuck IS. DES combustion modeling of a scramjet combustor. *AIAA Paper 2006-5097*, 2006.
28. Ingentio A, De Flora MG, Bruno C, Giacomazzi E, Steelant J. LES modeling of scramjet combustion. *AIAA Paper 2006-1383*, 2006.
29. Sung CJ, Li JG, Yu G, Law CK. Chemical kinetics and self ignition in a model supersonic hydrogen–air combustor. *AIAA Journal* 1999; **37**:208–214.
30. Just T, Schmalz F. Measurements of ignition delays of hydrogen–air mixtures under simulated conditions of supersonic combustion chambers. *AGARD CP No. 34*, *Part 2*, *Paper 19*, 1977.
31. Snyder AD, Robertson J, Zanders DL, Skinner FB. Shock tube studies of fuel-air ignition characteristics. *Report AFAPL-TR-65-93*, 1965.
32. Slack MW. Rate coefficient for $H+O_2+M=HO_2+M$ evaluated from shock tube measurements of induction times. *Combustion and Flame* 1977; **28**:241–249.
33. Bhaskaran KA, Gupta MC, Just T. Shock tube study of the effect of unsymmetric dimethyl hydrazine on the ignition characteristics of hydrogen–air mixtures. *Combustion and Flame* 1973; **21**:45–48.
34. Schultz E, Shepherd L. Validation of detailed reaction mechanisms for detonation simulation. *Explosion Dynamics Laboratory Report FM99-5*, 2000.
35. CANTERA. Object oriented software for reacting flows. Available from: http://www.cantera.org/.
36. Cheng TS, Wehrmeyer JA, Pitz RW, Jarrett O, Northam GB. Mixing enhancement in compressible mixing layers: an experimental study. *Combustion and Flame* 1994; **99**:157–173.
37. Burrow MC, Kurkov AP. An analytical and experimental study of supersonic combustion of hydrogen in vitiated air stream. *AIAA Journal* 1973; **11**:1217–1218.
38. Evans JS, Schexnayder CR, Beach HL. Application of a two-dimensional parabolic computer program to prediction of turbulent reacting flows. *NASA TP 1169*, 1978.
39. Drummond JP, Diskin GS, Cuttler AD. Fuel air mixing and combustion in scramjets. Technologies for Propelled Hypersonic Flight. *Final Report*, NATO Research and Technology Organization, Working Group AVT 10, 2001.
40. Cain T, Walton C. Review of experiments and flameholding in supersonic flow. *AIAA Paper 2002-3877*, 2002.
41. Gerlinger P, Brüggemann D. Multigrid convergence acceleration for turbulent supersonic flows. *International Journal for Numerical Methods in Fluids* 1997; **24**:1019–1035.
42. Gerlinger P, Brüggemann D. An implicit multigrid scheme for the compressible Navier–Stokes equations with low-Reynolds-number turbulence closure. *Journal of Fluids Engineering* 1998; **120**:257–262.
43. Gerlinger P. Investigation of an assumed PDF approach for finite-rate chemistry. *Combustion Science and Technology* 2003; **175**:841–872.
44. Gerlinger P, Noll B, Aigner M. Assumed PDF modeling and PDF structure investigation using finite-rate chemistry. *Progress in Computational Fluid Dynamics* 2005; **5**:334–344.
45. Jameson A, Yoon S. Lower–upper implicit schemes with multiple grids for the Euler equations. *AIAA Journal* 1987; **25**:929–935.
46. Shuen JS. Upwind differencing and LU factorization for chemical non-equilibrium Navier Stokes equations. *Journal of Computational Physics* 1992; **99**:233–250.
47. Coakley TJ, Huang PG. Turbulence modeling for high speed flows. *AIAA Paper 92-0436*, 1992.
48. Girimaji SS. Assumed β-pdf model for turbulent mixing: validation and extension to multiple scalar mixing. *Combustion Science and Technology* 1991; **78**:177–196.

DOI: 10.1002/fld

49. Möbus H, Gerlinger P, Brüggemann D. Scalar and joint scalar–velocity–frequency Monte Carlo PDF simulation of compressible of supersonic combustion. *Combustion and Flame* 2003; **132**:3–24.
50. Jarrett O, Cutler AD, Antcliff RR, Chitsomboom T, Dancey CL, Wang JA. Measurement of temperature, density and velocity in supersonic reacting flow for CFD code validation. *Twenty-fifth JANAF Combustion Meeting*, Huntsville, AI, vol. 1. CPIA Publication No. 498, CPIA Publication: Washington, DC, 1988; 357–364.
51. Boccanera M, Lentini D. Thermochemical closure for high speed flows. *Acta Astronautica* 2004; **55**:965–976.

DOI: 10.1002/fld